

# Process optimisation of the arc fusion splicing different types of single mode telecommunication fibres

M. RATUSZEK\*, Z. ZAKRZEWSKI, J. MAJEWSKI, and M.J. RATUSZEK

Institute of Telecommunications, University of Technology and Agriculture  
7 Kaliskiego Str., 85-796 Bydgoszcz, Poland

*Calculation method and coefficient values of the  $\text{GeO}_2$  dopant diffusion from the core to the cladding of spliced fibres in splicing temperature have been presented. Accepting different diffusion models, the intermediate area dimensions for various splicing parameters were calculated. A correlation between intermediate area parameters and splice loss of single mode fibres of different types including those designed for WDM has been discovered.*

*The analysis and usage of one-way OTDR measurement of splice losses of fibres with essential differences in cores diameters and numerical aperture has been presented. There also has been presented the influence of these parameters on one-way OTDR measurement of loss of splices of joined fibres.*

**Keywords:** diffusion, diffusion models, splice loss, telecommunication fibres, OTDR measurements.

## 1. Introduction

Optimisation of standard single mode fibre (SMF) splicing processes with erbium doped fibre (EDF) [1] revealed that significant splice loss, from a few dB to  $\approx 0.1$  dB, is obtained if a intermediate area arises within a splice due to erbium diffusing, Fig. 1.

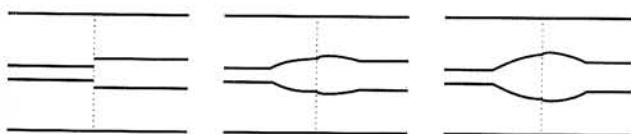


Fig. 1. Schematic presentation of dopant diffusion and arising of intermediate area.

EDF fibres are characterised by high numerical aperture (NA)  $\approx 0.25$ –0.3 and a small mode field diameter (MFD)  $\approx 4$ –6  $\mu\text{m}$  for  $\lambda = 1550$  nm. For SMF respectively MFD  $\approx 10$   $\mu\text{m}$  for  $\lambda = 1550$  nm, NA = 0.11–0.13. These parameters impose more difficult splicing condition than in case of splicing fibres: SMF, dispersion shifted – single mode fibre (DS-SMF), non zero dispersion shifted – single mode fibre (NZDS-SMF), depressed cladding – single mode fibre (DC-SMF), even though made according to different technologies. It is the result of smaller differences in NA of these fibres (from 0.11 to 0.17) as well as in MFD (from  $\approx 8$ –11  $\mu\text{m}$  for  $\lambda = 1550$  nm).

Concepts connected with arising of an intermediate area became a base for the optimisation of splicing conditions of

single mode fibres of different types, performed according to different technologies.

The main step of the splicing process is the basic splicing step (for the fusion splicer FSU 925RTC & FSU 975 it is the II step) in which the splicing temperature reaches the value  $\approx 2000^\circ\text{C}$ . For this temperature calculations of the intermediate area have been performed. Below the assumption for the optimisation for the optimisation process has been presented.

Different dopants ( $\text{GeO}_2$ , F) and their different levels of concentration in the core and the cladding cause the refraction coefficient change [2–4]. Higher  $\text{GeO}_2$  dopant level in the core leads to a bigger refraction coefficient difference between the core and the cladding, to a bigger numerical aperture NA and to a smaller mode field diameter MFD.

In the front of head connection of two one-mode fibres optical energy losses occur

$$A = 20 \log \frac{\omega_1^2 + \omega_2^2}{2\omega_1\omega_2}, \quad (1)$$

where A is the two fibres splice loss (dB),  $\omega_1$ ,  $\omega_2$  are the spliced fibres mode field radii.

In case of connecting fibres with the same MFDs, according to the Eq. (1) the splice loss is equal to zero assuming that the splice is centric splice loss. With this assumption of splice centricity and MFD adjusting, depends also on the difference in the numerical aperture NA, on the dopant type, its concentration in the cladding and the core [1]

\* e-mail: ratuszek@atr.bydgoszcz.pl

$$MFD = 2\omega = \frac{2a}{\sqrt{\ln[ka(NA)]}}, \quad (2)$$

where  $2a$  is the core diameter,  $NA$  is the numerical aperture, and

$$k = \frac{2\pi}{\lambda}.$$

Thus, in order to obtain levelling of mode fields for single mode fibres it is necessary to equalise diameters of the cores and numerical apertures of spliced fibres (dopant concentration) within the splice. Splice with low loss and good reflectance may be obtained when due to appropriate dopant diffusion in splice core, a proper intermediate area has been obtained, Fig.1 [1].

Obtaining an optical intermediate area is a function of time and splicing current [5].

Transient area optimisation as a function of splicing time and current may be performed knowing the  $\text{GeO}_2$  in  $\text{SiO}_2$  diffusion in splicing temperature.

## 2. $\text{GeO}_2$ w $\text{SiO}_2$ coefficient calculation method

In order to evaluate the diffusion processes  $\text{GeO}_2$ , a single mode fibre with  $NA = 0.217$  and content of germanium in the in the core  $C_{\text{GeO}_2} = 10.4 \text{ mol } \%$ , [6] and a quartz rod with the diameter  $\approx 130 \text{ } \mu\text{m}$  were used. Diffusion coefficients were calculated on the basis of changes, along splices, of luminescence profiles of the above mentioned spliced fibres. The splice temperature was  $2000^\circ\text{C}$  [7]. The time of the second step of splicing was changed from 1 to 6 seconds (Fig. 2). Linear dependence of thermoluminescence on  $\text{GeO}_2$  concentration in  $\text{SiO}_2$  was assumed [8]. The curves of luminescence intensity changes for different splicing times as a function of the distance from the splice front have been shown in Fig. 3 [6,7].

For the purpose of calculation of the diffusion coefficient the below mentioned conditions and parameters have been assumed:

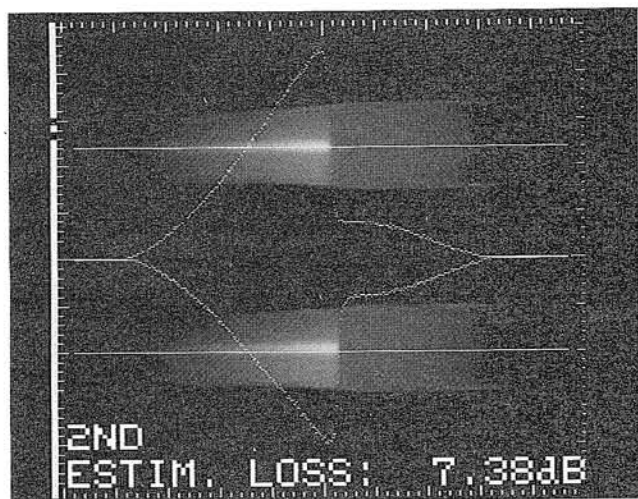


Fig. 2. Exemplary thermoluminescence intensity profile for  $t = 6 \text{ s}$ .

- diffusion from unlimited dopant source, i.e.,  $N(0,t) = N_0$ ,
- initial concentration inside the quartz rod is small in comparison with  $N_0$ .

Thus,  $\text{GeO}_2$  concentration in the quartz rod may be rendered by the following expression

$$N(x,t) = N_0 \operatorname{erfc} \frac{x}{2\sqrt{Dt}}. \quad (3)$$

Density of  $\text{SiO}_2$   $\rho = 2.20 \text{ g/cm}^3$  has been assumed. Content  $C_{\text{GeO}_2} = 10.4 \text{ mol } \%$  corresponds with the concentration of  $\text{GeO}_2$  in  $\text{SiO}_2$ ,  $N_0 = 2.27 \times 10^{21} \text{ cm}^{-3}$ . With  $N_0$ ,  $x$ ,  $t$  being known,  $N(x,t)$  being evaluated on the basis of luminescence, the diffusion coefficient values  $D$  for germanium in  $\text{SiO}_2$  at the temperature  $\approx 2000^\circ\text{C}$  has been estimated. The coefficients were calculated for the distance  $x = 7.5 \text{ } \mu\text{m}$  and  $x = 12.5 \text{ } \mu\text{m}$  from the splice front. Values obtained were changing in the range from  $D = 3 \times 10^{-7} \text{ cm}^2/\text{s}$  to  $D = 2 \times 10^{-6} \text{ cm}^2/\text{s}$ . Higher coefficient values were obtained for shorter splicing times and smaller distances from the splice front. Dopant diffusion coefficients can be rendered by the following equation [9]

$$D = D_\infty \exp\left(\frac{-E_a}{kT}\right), \quad (4)$$

where  $D_\infty$  is the diffusion coefficient for  $T = \infty$ ,  $E_a$  is the dopant activation energy in  $\text{SiO}_2$ .

Having accepted theoretical values  $E_a$  [6,9] for inter-atomic dopants  $E_{a1} \approx 1 \text{ eV}$  and diffusing dopants by means of substituting  $E_{a2} = 3.0 \text{ eV}$  values of  $D_\infty$  where calculated. For  $E_{a2}$ :  $D_\infty = 20\text{--}130 \text{ cm}^2/\text{s}$ , for  $E_{a1}$ : from  $D_\infty = 1.2 \times 10^{-4} \text{ cm}^2/\text{s}$  to  $D_\infty = 8 \times 10^{-4} \text{ cm}^2/\text{s}$ . The calculated values  $D_\infty$  for  $E_{a1}$  are close to the theoretical value  $D_\infty = 1.7 \times 10^{-3} \text{ cm}^2/\text{s}$  [9].

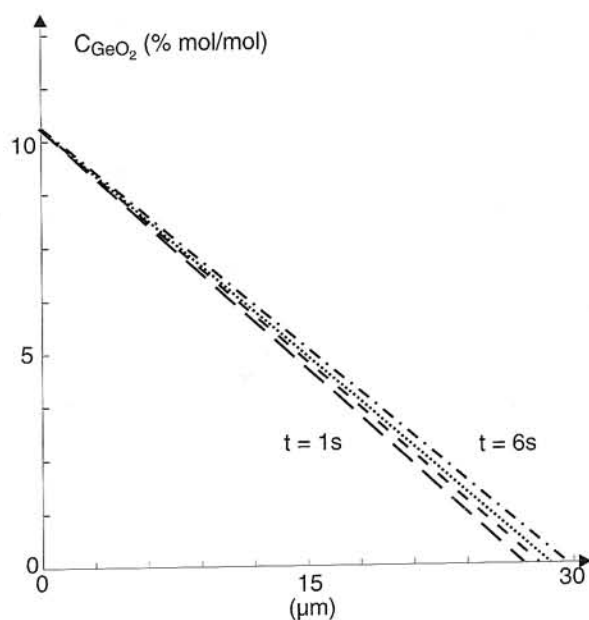


Fig. 3. Thermoluminescence intensity changes and assignment of  $\text{GeO}_2$  in  $\text{SiO}_2$  concentration for different splicing times in the distance from the splice front function.

In literature there is no information about values of diffusion coefficient  $\text{GeO}_2$  in  $\text{SiO}_2$  in temperature  $2000^\circ\text{C}$ . Theoretically foreseeable diffusion coefficient for interatomic dopant in  $\text{SiO}_2$  for  $1000^\circ\text{C}$  is  $D = 4.1 \times 10^{-7} \text{ cm}^2/\text{s}$  [9]. Using Eq. (4) theoretical value of diffusion coefficient in temperature  $2000^\circ\text{C}$  is  $D = 2.6 \times 10^{-5} \text{ cm}^2/\text{s}$  and it is higher than estimated value of diffusion coefficient in this paper.

### 3. Simulation of diffusion process in splice intermediate area

In the intermediate area there occurs levelling of the dopant concentration in the core and partly in spliced fibres claddings. Literature and catalogue data for fibres do not contain information about  $\text{GeO}_2$  concentration in the cores. Thus, an appropriate dopant concentration had to be assigned to numerical aperture NA so that the dopant concentration in the cores during splicing fibres with different NA could be known. It gives us a possibility to estimate the diffusion time needed for dopant concentration levelling in spliced fibres, subsequently the splicing time.

The results of this assignment have been shown in Fig. 4. For calculations, refraction coefficient values were accepted,  $n$  for  $\lambda = 1310 \text{ nm}$  and  $\lambda = 1550 \text{ nm}$ , depending on mole concentration of  $\text{GeO}_2$  in  $\text{SiO}_2$  presented in Ref. 4, Fig. 4. For not doped  $\text{SiO}_2$   $n = 1.4468$  for  $\lambda = 1310 \text{ nm}$  and  $n = 1.4440$  for  $\lambda = 1550 \text{ nm}$  have been accepted. It was estimated that  $1 \text{ mol } \% \text{ GeO}_2$  in  $\text{SiO}_2$  corresponds with  $\text{GeO}_2$  dopant concentration equal to  $N_0 = 2.19 \times 10^{20} \text{ cm}^{-3}$  and respectively  $10 \text{ mol } \% \text{ GeO}_2$  in  $\text{SiO}_2$  and  $N_0 = 2.19 \times 10^{21} \text{ cm}^{-3}$ . Numerical aperture value NA was calculated from the expression

$$NA = n_1 \sqrt{2\Delta}, \quad (5)$$

where  $\Delta = (n_1 - n_2)/n_1$ ,  $n_1$  is the core refraction coefficient,  $n_2$  is the cladding refraction coefficient.

Figure 4 allows directly evaluating the  $\text{GeO}_2$  dopant concentration in fibres, which significantly differ in respect of their parameters.

- |   |                    |
|---|--------------------|
| 1. $N_0 = 2.27 \times 10^{20} \text{ cm}^{-3}$  | (NA $\cong$ 0.08)  |
| 2. $N_0 = 5.00 \times 10^{20} \text{ cm}^{-3}$  | (NA $\cong$ 0.105) |
| 3. $N_0 = 1.00 \times 10^{21} \text{ cm}^{-3}$  | (NA $\cong$ 0.15)  |
| 4. $N_0 = 2.27 \times 10^{21} \text{ cm}^{-3}$  | (NA $\cong$ 0.22)  |
|   |                    |
| 5. $N_0 = 2.27 \times 10^{20} \text{ cm}^{-3}$  | (NA $\cong$ 0.08)  |
| 6. $N_0 = 5.00 \times 10^{20} \text{ cm}^{-3}$  | (NA $\cong$ 0.105) |
| 7. $N_0 = 1.00 \times 10^{21} \text{ cm}^{-3}$  | (NA $\cong$ 0.15)  |
| 8. $N_0 = 2.27 \times 10^{21} \text{ cm}^{-3}$  | (NA $\cong$ 0.22)  |
|   |                    |
| 9. $N_0 = 2.27 \times 10^{20} \text{ cm}^{-3}$  | (NA $\cong$ 0.08)  |
| 10. $N_0 = 5.00 \times 10^{20} \text{ cm}^{-3}$ | (NA $\cong$ 0.105) |
| 11. $N_0 = 1.00 \times 10^{21} \text{ cm}^{-3}$ | (NA $\cong$ 0.15)  |
| 12. $N_0 = 2.27 \times 10^{21} \text{ cm}^{-3}$ | (NA $\cong$ 0.22)  |

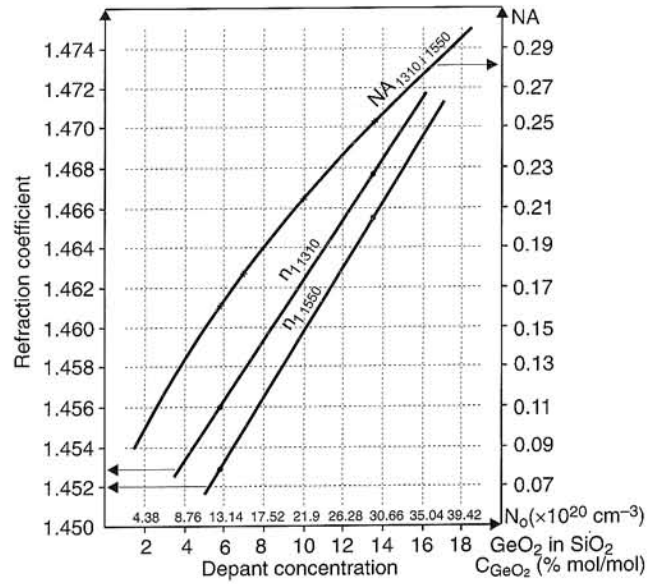


Fig. 4. Dependencies of refraction coefficient and numerical apertures NA on  $\text{GeO}_2$  concentration in  $\text{SiO}_2$ .

### 3.1 $\text{GeO}_2$ in $\text{SiO}_2$ diffusion process simulation in intermediate area for diffusion from unlimited dopant source

If the following conditions are fulfilled [9]

- dopant concentration in the core during the diffusion process (splicing) is accepted to be a constant, that is
- $$N(0, t) = N_0, \quad (6)$$
- initial dopant concentration in the cladding is small in comparison with  $N_0$ , i.e.,

$$N(x > 0, 0) = 0, \quad (7)$$

then dopant concentration distribution is described by the following expression [9]:

$x = 0-15 \mu\text{m}$		
$D = 3 \times 10^{-7} \frac{\text{cm}^2}{\text{s}}$		$t = 1, 2, 3, 4, 5 \text{ s}$
		$t = 1, 2, 3, 4, 5 \text{ s}$
		$t = 1, 2, 3, 4, 5 \text{ s}$
		$t = 1, 2, 3, 4, 5 \text{ s}$
$D = 7 \times 10^{-7} \frac{\text{cm}^2}{\text{s}}$		$t = 1, 2, 3, 4, 5 \text{ s}$
		$t = 1, 2, 3, 4, 5 \text{ s}$
		$t = 1, 2, 3, 4, 5 \text{ s}$
		$t = 1, 2, 3, 4, 5 \text{ s}$
$D = 2 \times 10^{-6} \frac{\text{cm}^2}{\text{s}}$		$t = 1, 2, 3, 4, 5 \text{ s}$
		$t = 1, 2, 3, 4, 5 \text{ s}$
		$t = 1, 2, 3, 4, 5 \text{ s}$
		$t = 1, 2, 3, 4, 5 \text{ s}$

$$N(x,t) = N_o \operatorname{erfc} \frac{x}{2\sqrt{Dt}} \quad (8)$$

$$\operatorname{erfc}(x) = 1 - \operatorname{erf}(x)$$

Calculations for the  $\text{GeO}_2$  in  $\text{SiO}_2$  distributions during splicing process for diffusion from an unlimited dopant source, have been performed for the data shown above.

Exemplary results of  $N(x,t)$   $\text{GeO}_2$  in  $\text{SiO}_2$  dopant concentration distribution for diffusion from unlimited dopant source have been presented in Figs. 5 and 6.

### 3.2 $\text{GeO}_2$ in $\text{SiO}_2$ diffusion process simulation in splice intermediate area for diffusion from layer with limited thickness

For in the moment  $t = 0$  the dopant concentration diffusion is described [9]:

$$N(x,0) = \begin{cases} N_0 & -h < x < 0 \\ 0 & -h > x > 0 \end{cases} \quad (9)$$

which means that the core diameter  $2a = 0 - h = h$ , then after the time  $t$  dopant concentration distribution will be accounted for by the expression

$$N(x,t) = \frac{N_o}{2} \left[ \operatorname{erf} \left( \frac{x+h}{2\sqrt{Dt}} \right) - \operatorname{erf} \left( \frac{x}{2\sqrt{Dt}} \right) \right] \quad (10)$$

Expression (9) can be applied, e.g., for approximate dopant diffusion calculation from the so called finished

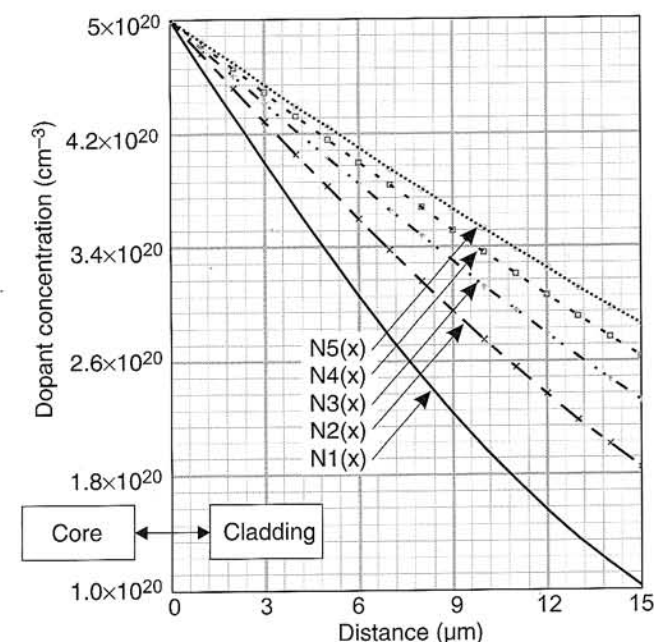


Fig. 5.  $\text{GeO}_2$  in  $\text{SiO}_2$  concentration distribution within the splice for diffusion from an unlimited source and parameters;  $x = 0 - 15 \mu\text{m}$ ,  $t_1 = 1\text{s}$ ,  $t_2 = 2\text{s}$ ,  $t_3 = 3\text{s}$ ,  $t_4 = 4\text{s}$ ,  $t_5 = 5\text{s}$ ,  $N_o = 5 \times 10^{20} \text{ cm}^{-3}$ ,  $D = 7 \times 10^{-7} \text{ cm}^2/\text{s}$ .

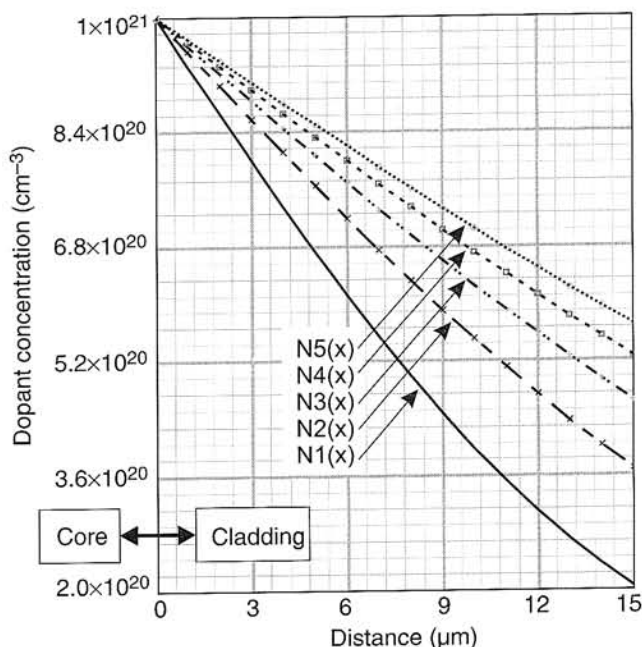


Fig. 6.  $\text{GeO}_2$  in  $\text{SiO}_2$  concentration distribution within the splice for diffusion from an unlimited source and parameters;  $x = 0 - 15 \mu\text{m}$ ,  $t_1 = 1\text{s}$ ,  $t_2 = 2\text{s}$ ,  $t_3 = 3\text{s}$ ,  $t_4 = 4\text{s}$ ,  $t_5 = 5\text{s}$ ,  $N_o = 1 \times 10^{21} \text{ cm}^{-3}$ ,  $D = 7 \times 10^{-7} \text{ cm}^2/\text{s}$ .

layer, i.e., the dopant concentration distribution from the core to the cladding may be simulated, since the core may be treated as a specific "finished" layer  $\text{SiO}_2 + \text{GeO}_2$  in pure  $\text{SiO}_2$ , that in the cladding. In this case the core is a limited dopant source which means that  $\text{GeO}_2$  concentration decreases in the core which the diffusion time and temperature increase.

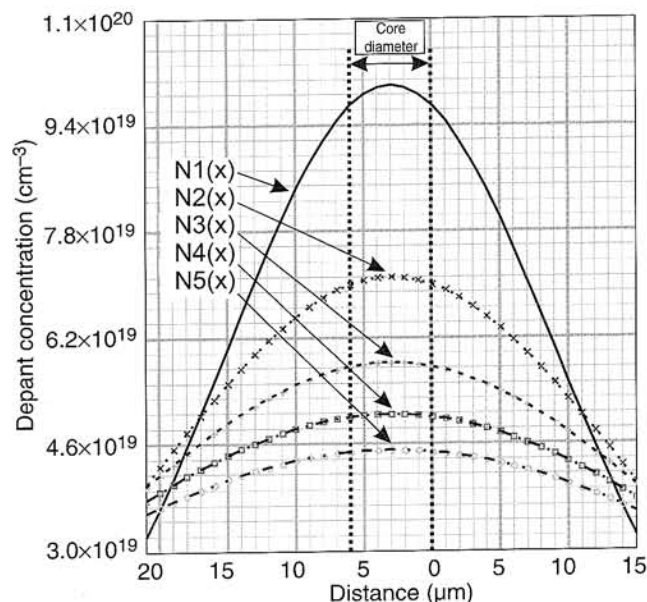


Fig. 7.  $\text{GeO}_2$  in  $\text{SiO}_2$  concentration distribution within splice for distribution from the layer with finished thickness and parameters;  $x = -21 - 15 \mu\text{m}$ ,  $t_1 = 1\text{s}$ ,  $t_2 = 2\text{s}$ ,  $t_3 = 3\text{s}$ ,  $t_4 = 4\text{s}$ ,  $t_5 = 5\text{s}$ ,  $h = 6 \mu\text{m}$ ,  $N_o = 5 \times 10^{20} \text{ cm}^{-3}$ ,  $D = 7 \times 10^{-7} \text{ cm}^2/\text{s}$ .



1. $N_0 = 2.27 \times 10^{20} \text{ cm}^{-3}$ (NA $\cong 0.08$ )	$D = 3 \times 10^{-7} \frac{\text{cm}^2}{\text{s}}$	$t = 1, 2, 3, 4, 5 \text{ s}$	$h = 6 \text{ and } 9 \mu\text{m}$
2. $N_0 = 5.00 \times 10^{20} \text{ cm}^{-3}$ (NA $\cong 0.105$ )		$t = 1, 2, 3, 4, 5 \text{ s}$	
3. $N_0 = 1.00 \times 10^{21} \text{ cm}^{-3}$ (NA $\cong 0.15$ )		$t = 1, 2, 3, 4, 5 \text{ s}$	
4. $N_0 = 2.27 \times 10^{21} \text{ cm}^{-3}$ (NA $\cong 0.22$ )		$t = 1, 2, 3, 4, 5 \text{ s}$	
5. $N_0 = 2.27 \times 10^{20} \text{ cm}^{-3}$ (NA $\cong 0.08$ )		$t = 1, 2, 3, 4, 5 \text{ s}$	
6. $N_0 = 5.00 \times 10^{20} \text{ cm}^{-3}$ (NA $\cong 0.105$ )	$D = 7 \times 10^{-7} \frac{\text{cm}^2}{\text{s}}$	$t = 1, 2, 3, 4, 5 \text{ s}$	$h = 6 \text{ and } 9 \mu\text{m}$
7. $N_0 = 1.00 \times 10^{21} \text{ cm}^{-3}$ (NA $\cong 0.15$ )		$t = 1, 2, 3, 4, 5 \text{ s}$	
8. $N_0 = 2.27 \times 10^{21} \text{ cm}^{-3}$ (NA $\cong 0.22$ )		$t = 1, 2, 3, 4, 5 \text{ s}$	
9. $N_0 = 2.27 \times 10^{20} \text{ cm}^{-3}$ (NA $\cong 0.08$ )		$t = 1, 2, 3, 4, 5 \text{ s}$	
10. $N_0 = 5.00 \times 10^{20} \text{ cm}^{-3}$ (NA $\cong 0.105$ )		$t = 1, 2, 3, 4, 5 \text{ s}$	
11. $N_0 = 1.00 \times 10^{21} \text{ cm}^{-3}$ (NA $\cong 0.15$ )	$D = 2 \times 10^{-6} \frac{\text{cm}^2}{\text{s}}$	$t = 1, 2, 3, 4, 5 \text{ s}$	$h = 6 \text{ and } 9 \mu\text{m}$
12. $N_0 = 2.27 \times 10^{21} \text{ cm}^{-3}$ (NA $\cong 0.22$ )		$t = 1, 2, 3, 4, 5 \text{ s}$	

This model renders, in a better way, real processes that take place in splice fibres as in reality the core is not an unlimited  $\text{GeO}_2$  dopant source.

Calculations have been made for the below-presented data

- $x = -21$ – $15 \mu\text{m}$   
 $h = 6 \mu\text{m}$  (for DS-SMF) core diameter in figures from  $-6$  to  $0 \mu\text{m}$   
 $h = 9 \mu\text{m}$  (for SMF) core diameter in figures from  $-9$  to  $0 \mu\text{m}$

Exemplary results of dopant  $N(t, x)$ , i.e.,  $\text{GeO}_2$  in  $\text{SiO}_2$  distribution calculation for diffusion from a layer with finished thickness for the data and  $h = 6 \mu\text{m}$  have been presented in Figs. 7 and 8.

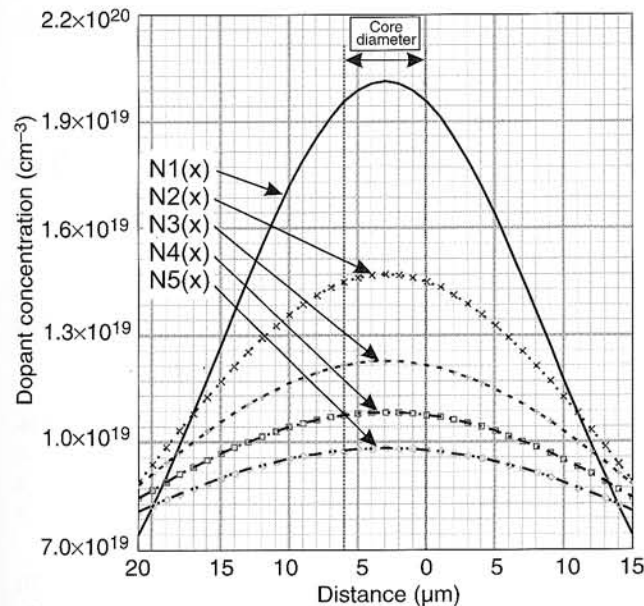


Fig. 8.  $\text{GeO}_2$  in  $\text{SiO}_2$  concentration distribution within splice for diffusion from the layer with finished thickness and parameters;  $x = -21$ – $15 \mu\text{m}$ ,  $t_1 = 1 \text{ s}$ ,  $t_2 = 2 \text{ s}$ ,  $t_3 = 3 \text{ s}$ ,  $t_4 = 4 \text{ s}$ ,  $t_5 = 5 \text{ s}$ ,  $h = 6 \mu\text{m}$ ,  $N_0 = 1 \times 10^{21} \text{ cm}^{-3}$ ,  $D = 7 \times 10^{-7} \text{ cm}^2/\text{s}$ .

#### 4. Diffusion processes – summary

In splicing connecting practice extreme differences of core diameters (mode field) and numerical apertures are  $\Delta(2a) \cong 2$ – $3 \mu\text{m}$  and  $\Delta(\text{NA}) \cong 0.05$ – $0.06$ , and concerns spliced fibres with shifted dispersion DS-SMF to III optical window as well as standard SMF with zero dispersion in II optical window. It corresponds with dopant concentration  $N_0 = 5 \times 10^{20} \text{ cm}^{-3}$  (NA  $\cong 0.105$ ) fibres SMF and  $N_0 = 1 \times 10^{21} \text{ cm}^{-3}$  (NA  $\cong 0.15$ ) fibres DS-SMF. For these concentrations and different diffusion coefficient, long splicing times in II are the most advantageous during the main splicing step – diffusion model from an unlimited source. For long splicing times there occurs levelling of the dopant concentration in spliced fibres along distances which are differences in core diameters. Evidently splicing times can not be prolonged to infinity as it weakens the splice, and may as well lead to melting instead of splicing the fibres.

Diffusion takes place under the influence of dopant concentration gradient. Thus, diffusion within the splice of spliced fibres will be directed from the core to its claddings and from the core of the fibre with higher dopant concentration (in practice it refers to fibres with bigger NA and smaller core diameter  $2a$ ) toward the core of fibres with lower dopant concentration – this effect is not taken into account in the simulation process, Fig. 9.

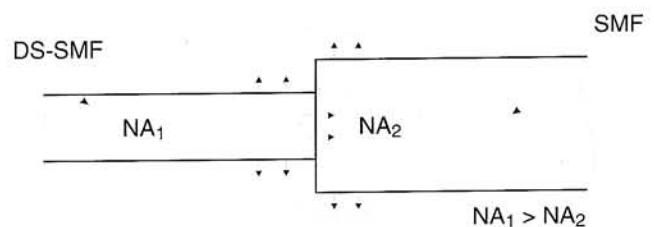


Fig. 9. Diffusion directions in spliced fibres within the splice.

This means that the dopant diffusion from the core in a fibre with lower dopant concentration will be in reality much smaller than it result from, e.g., Fig. 7, SMF fibres with NA  $\cong 0.11$  and  $N_0 \cong 5 \times 10^{20} \text{ cm}^{-3}$  – a model of diffusion from a layer with finished thickness.

Therefore, the dopant concentration within the splice in a fibre with a lower NA will be comparable or not much lower (diffusion to the cladding) than the concentration level before diffusion, i.e., for short diffusion times then, the dopant concentration levelling conditions within the splice, e.g., for DS-SMF (NA  $\approx$  0.16,  $N_0 \approx 1 \times 10^{21} \text{ cm}^{-3}$ , Fig. 8) and SMF (NA  $\approx$  0.11,  $N_0 \approx 5 \times 10^{20} \text{ cm}^{-3}$ , Fig. 7) fibres occur as well – conclusions for the diffusion from an unlimited dopant source for times 4, 5 seconds and from  $D = 3 \times 10^{-7} \text{ cm}^2/\text{s}$  to  $D = 2 \times 10^{-6} \text{ cm}^2/\text{s}$ . That means, fundamental fusion time (step II for FSU 925 RTC) must be from 4 to 5 seconds with the splicing temperature assumption  $\approx 2000^\circ\text{C}$ . Our experience in splicing of SMF, DC-SMF, DS-SMF and NZDS-SMF fibres in different splicing combinations revealed that applying the above presented conclusions we may obtain repeatable splices with the loss  $A \leq 0.08 \text{ dB}$  and with unnoticeable reflectance [5].

## 5. Analysis of one-way OTDR measurements of splice loss for telecommunication fibre with different parameters

Analysis of one way measurement is an underestimated part of reflectometric measurements. Its importance will certainly increase since now we are going to have more frequent contacts with one-way accessible fibre routes. So far reflectometric one way values for splice loss of single mode fibres of different types have not been defined yet. Loss value  $A_{12}$  ( $A_{21}$ ) for single mode SMF standard should not exceed 0.6 dB [10].

### 5.1. Real and apparent splice loss in OTDR measurements

According to Ref. 11, the backscattered power detected by OTDR from a point immediately preceding the splice is give by

$$P_1 = P_o S_1 \exp(-2\alpha_1 L_1), \quad (11)$$

where  $P_o$  is the initial power level (dBm),  $L_1$  is the fibre length (km),  $\alpha_1$  is the attenuation coefficient (dB/km),  $S_1$  is the backscatter coefficient, the latter being given by [2]

$$S_1 = 0.038 \left( \frac{\lambda}{n_1 \omega_1} \right)^2, \quad (12)$$

where  $\lambda$  is the wavelength,  $\omega_1$  is the mode field radius,  $n_1$  is the core refractive index. The subscript 1 refers to the input fibre.

The backscattered power detected by OTDR from a point immediately following the splice is give by [11]

$$P_2 = P_o S_2 T_{12} T_{21} \exp(-2\alpha_1 L_1), \quad (13)$$

where  $T_{12}$  is the splice transmission value in the forward direction, and  $T_{21}$  the corresponding quantity in the reverse direction. With the assumption of central fibre connection fixing [11]

$$T_{12} = T_{21} = 4 \left( \frac{\omega_1 \omega_2}{\omega_1^2 + \omega_2^2} \right)^2, \quad (14)$$

$S_2$  as the backscatter coefficient of fibre behind the splice is given by

$$S_2 = 0.038 \left( \frac{\lambda}{n_2 \omega_2} \right)^2, \quad (15)$$

where the subscript 2 refers to the output fibre.

One-way  $A_{12}$  fibre loss from  $1 \rightarrow 2$  is

$$2A_{12} = 10 \log \frac{P_1}{P_2}. \quad (16)$$

Thus, applying Eqs. (1), (2), and (4) we obtain

$$\frac{P_1}{P_2} = \left( \frac{n_2 \omega_2}{n_1 \omega_1} \right)^2 \frac{1}{T_{12} T_{21}}, \quad (17)$$

$$2A_{12} = 10 \log \frac{P_1}{P_2} = 20 \log \frac{n_2}{n_1} + 20 \log \frac{\omega_2}{\omega_1} + 40 \log \left[ \frac{1}{2} \left( \frac{\omega_1}{\omega_2} + \frac{\omega_2}{\omega_1} \right) \right] \quad (18)$$

Hence, one-way apparent splice loss in the direction  $1 \rightarrow 2$  is

$$A_{12} = 10 \log \frac{n_2}{n_1} + 10 \log \frac{\omega_2}{\omega_1} + 20 \log \left[ \frac{1}{2} \left( \frac{\omega_1}{\omega_2} + \frac{\omega_2}{\omega_1} \right) \right]. \quad (19)$$

And similarly one-way apparent splice loss from  $2 \rightarrow 1$  is

$$A_{21} = 10 \log \frac{n_1}{n_2} + 10 \log \frac{\omega_1}{\omega_2} + 20 \log \left[ \frac{1}{2} \left( \frac{\omega_1}{\omega_2} + \frac{\omega_2}{\omega_1} \right) \right]. \quad (20)$$

Real splice loss is an arithmetic mean of (9) and (10) including signs  $A_{12}$  and  $A_{21}$

$$A = \frac{A_{12} + A_{21}}{2} = 20 \log \left[ \frac{1}{2} \left( \frac{\omega_1}{\omega_2} + \frac{\omega_2}{\omega_1} \right) \right]. \quad (21)$$

Analysis of Eqs. (19), (20), and (21) lets us conclude that 10% difference of spliced fibre mode fields provides one-way  $A_{12} \approx 0.45$  dB whereas in reality the loss in such a case is  $A = 0.05$  dB.

In one-way measurements the component  $10\log(n_1/n_2)$ , even with extremely big refractive coefficient differences, e.g.,  $n_1 = 1.47$  and  $n_2 = 1.45$ , is 0.059 dB, and it slightly changes values  $A_{12}$  and  $A_{21}$ . However, differences in mode fields, e.g.,  $2\omega_{1550\text{ nm}} = 8.5 \mu\text{m}$  (for DS-SMF) and  $2\omega_{21550\text{ nm}} = 10.5 \mu\text{m}$  (for SMF) give the following values  $A_{12}$  and  $A_{21}$  (components  $10\log(n_1/n_2)$  and  $10\log(n_1/n_2)$  have been left out):  $A_{12} = 1.11$  dB and  $A_{21} = -0.725$  dB. Whereas the real loss is  $A = 0.192$  dB. Thus, one-way fibre splice loss values, which significantly differ in respect of their mode field diameters, may theoretically reveal values, which significantly exceed 1 dB.

## 5.2. Experimental results of one-way loss measurements of splice which differ significantly in respect of core diameters and numerical apertures

Non zero dispersion shifted single mode fibre NZDS-SMF of the TrueWave® type and standard single mode fibre SMF of Lycom have been used for testing. Both fibres were made (produced) according to MCVD technology.

For SMF – Lycom:  $NA \approx 0.12$ ,  
 $2a \approx 8 \mu\text{m}$ ,  
 $2\omega_{1550\text{ nm}} = 10.5 \mu\text{m}$ .

For NZDS TrueWave®:  $NA = 0.154$ ,  
 $2a = 5.62 \mu\text{m}$ ,  
 $2\omega_{21550\text{ nm}} = 8.24 \mu\text{m}$ .

Splices were performed with changing the second, basic splicing step for FSU 925RTC Ericsson fusion splicer, the following parameters have been changed:

1.  $t_2 = 1.5$  s for  $I_2 = 15, 16, 17, 18$  mA;
2.  $t_2 = 2.0$  s for  $I_2 = 15, 16, 17, 18$  mA;
3.  $t_2 = 3.0$  s for  $I_2 = 15, 16, 17, 18$  mA;
4.  $t_2 = 4.0$  s for  $I_2 = 15, 16, 17, 18$  mA;
5.  $t_2 = 5.0$  s for  $I_2 = 15, 16, 17, 18$  mA.

Results of one-way measurements  $A_{12}$  (from SMF–Lycom to NZDS TrueWave®) and  $A_{21}$  (from TrueWave® to Lycom), and real splice loss  $A = (A_{12} + A_{21})/2$  for  $\lambda = 1310$  nm and  $\lambda = 1550$  nm were shown in Figs. 10–14.

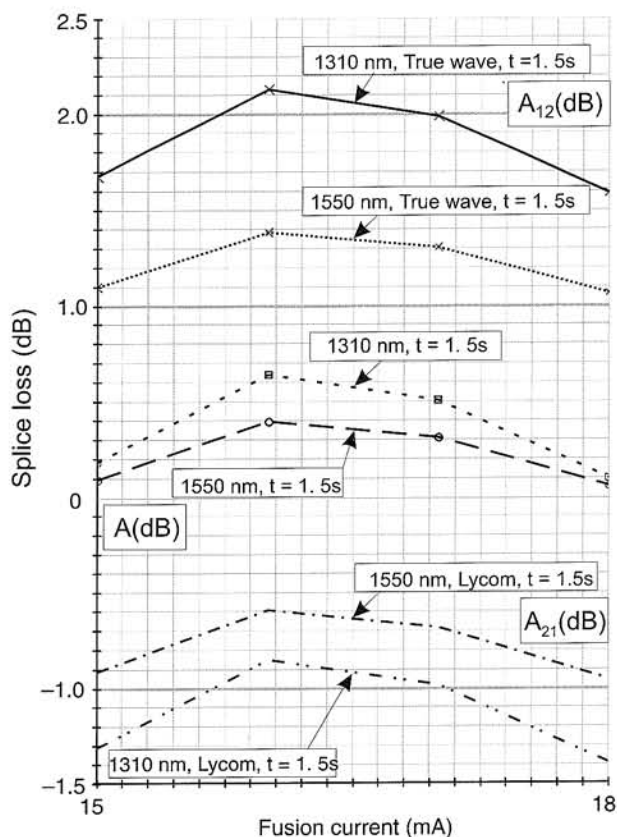


Fig. 10. Splice loss measurement results  $A_{12}$ ,  $A_{21}$  and  $A$  for  $\lambda = 1310$  nm,  $\lambda = 1550$  nm in the fusion current function with  $t_2 = 1.5$  s.

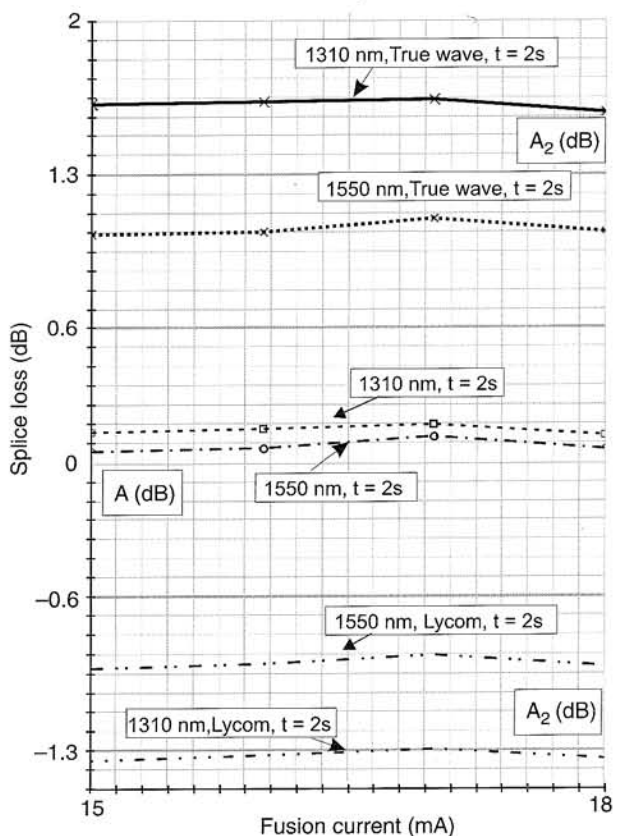


Fig. 11. Splice loss measurement results  $A_{12}$ ,  $A_{21}$ , and  $A$  for  $\lambda = 1310$  nm,  $\lambda = 1550$  nm in the fusion current function with  $t_2 = 2$  s.

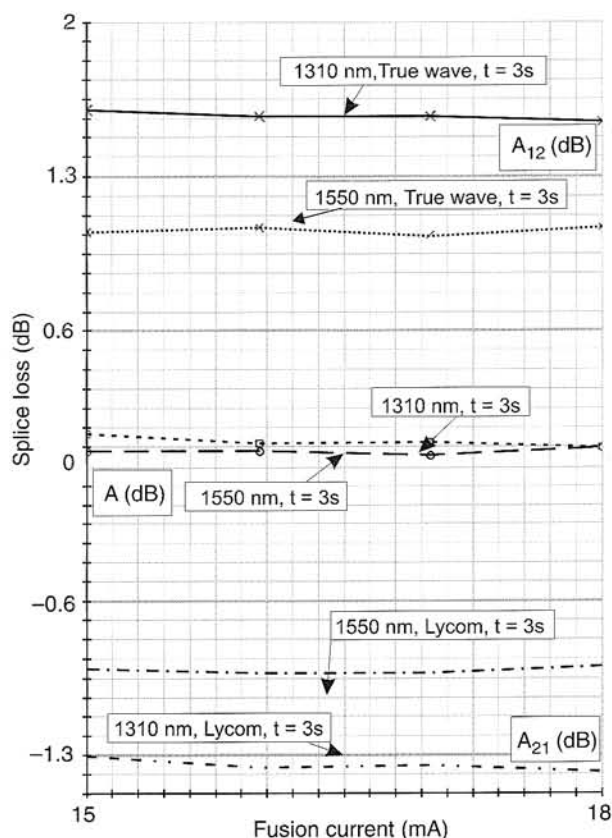


Fig. 12. Splice loss measurement results  $A_{12}$ ,  $A_{21}$  and  $A$  for  $\lambda = 1310$  nm,  $\lambda = 1550$  nm in the fusion current function with  $t_2 = 3$  s.

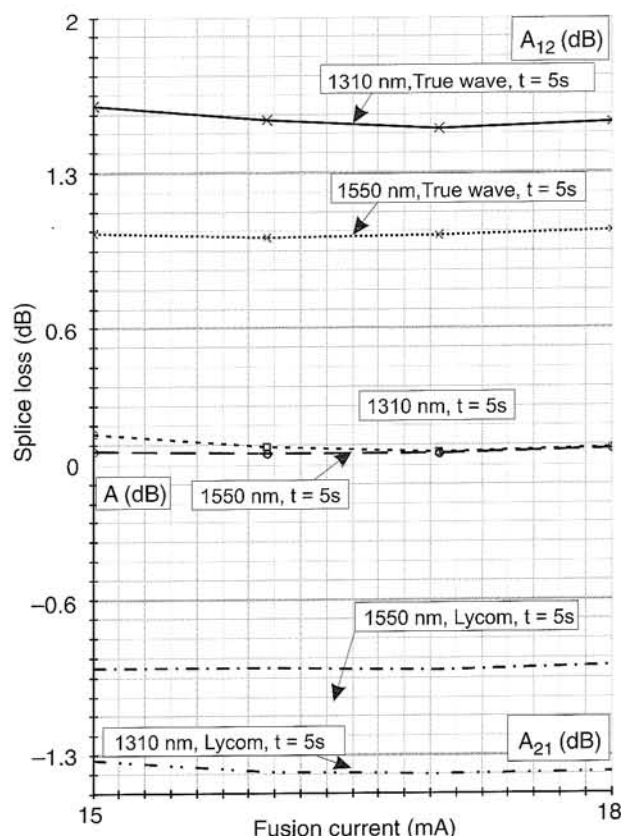


Fig. 14. Splice loss measurement results  $A_{12}$ ,  $A_{21}$  and  $A$  for  $\lambda = 1310$  nm,  $\lambda = 1550$  nm in the fusion current function with  $t_2 = 5$  s.

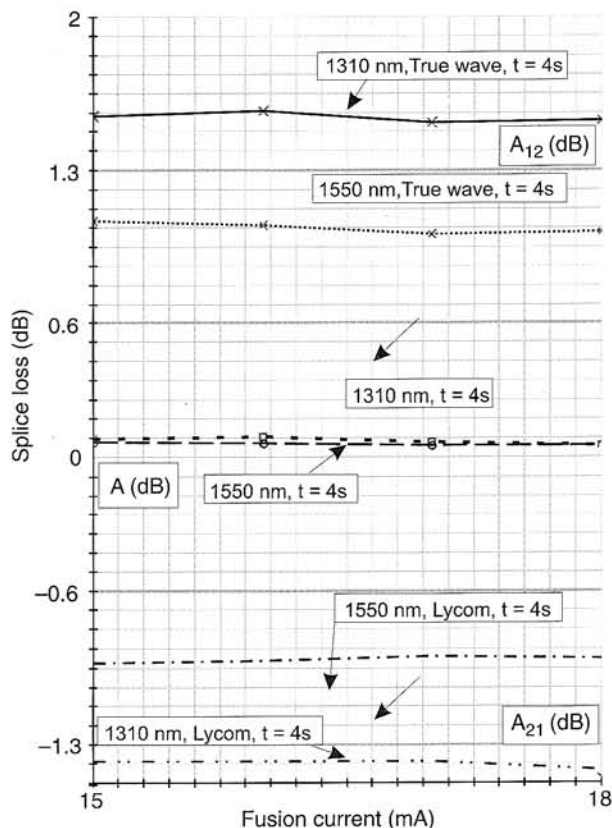


Fig. 13. Splice loss measurement results  $A_{12}$ ,  $A_{21}$  and  $A$  for  $\lambda = 1310$  nm,  $\lambda = 1550$  nm in the fusion current function with  $t_2 = 4$  s.

## 6. Anomalies in reflectometric splice loss measurements for telecommunication fibres of different types for $\lambda = 1310$ nm and $\lambda = 1550$ nm and their interpretations

Along with the increase of splicing current a signification decreases of  $|A_{21}|$  and  $A_{12}$  was expected. Such an assumption resulted from the presented tests [5] concerning the transient area, i.e., faster levelling of spliced fibre mode fields during splicing due to temperature increase. During levelling of  $\omega_1$  and  $\omega_2$  according to (9) and (10) apparent values  $|A_{21}|$  and  $A_{12}$  should decrease and  $A$  should, of course, decrease as well simulation of such a process has been shown in Fig. 15.

The experiment shows that up from certain splicing temperatures does not increase significantly. Therefore, for defined currents with the use of which the splicing temperature is  $\approx 2000^\circ\text{C}$  the most important is the splicing time. In the experiment we accept:  $t_2 \geq 4$  s and  $I_2 \geq 17$  mA.

Why, then in the one-way measurement experiment  $\log(\omega_1/\omega_2) \neq \log(\omega_2/\omega_1)$  something which needs to be explained, in spite of the fact that  $A$  loss decreases, Figs. 1–5, which means that  $\omega_2$  approaches  $\omega_1$ .

With comparable core diameter and numerical apertures NA of spliced fibres, splice loss is bigger for  $\lambda = 1550$  nm



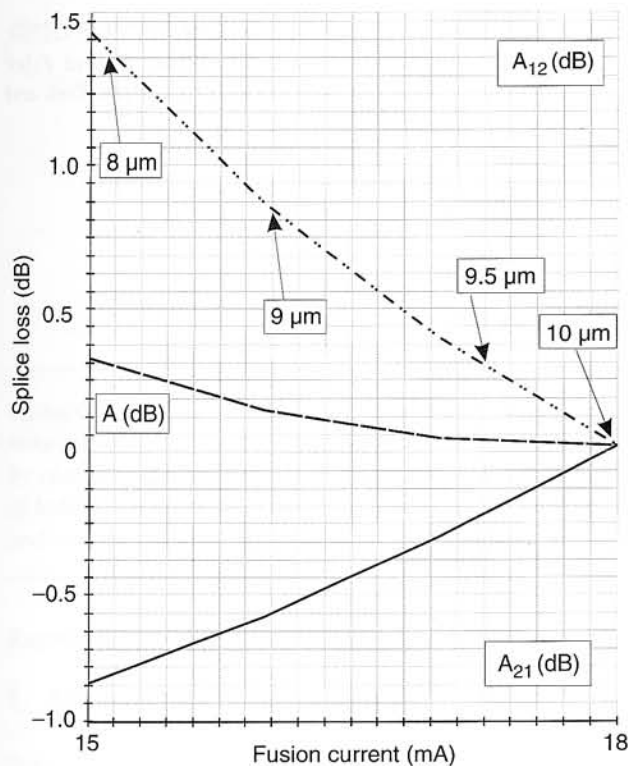


Fig. 15. Calculated loss  $A_{12}$ ,  $A_{21}$ , and  $A$  on the basis of Eqs. (9)–(11).  $\omega_2 = 10 \mu\text{m}$  (for all currents),  $\omega_1 = 8\text{--}10 \mu\text{m}$  (for  $I_2 = 15\text{--}18 \text{ mA}$ ) have been assigned to fusion current.

then  $\lambda = 1310 \text{ nm}$ . It results from the fact that the mode field for  $\lambda = 1550 \text{ nm}$  is bigger. This means that the defect field which is the splice, is bigger for  $\lambda = 1550 \text{ nm}$  which brings about a higher optical power loss. This phenomenon is not explicitly accounted for in Eq. (21).

Splice loss in fibres significantly differing in respect of core diameters and numerical apertures NA, on the contrary show higher values  $A$  for  $\lambda = 1310 \text{ nm}$  than for  $\lambda = 1550 \text{ nm}$ , Figs. 10–14. It refers especially to non-optimised splices. For optimised ones, i.e., for higher  $t_2$  and  $I_2$ , these differences are smaller, coming down to zero, Figs. 10–14. Inverse loss dependency, which determines fusion time  $t_2$  and fusion current  $I_2$ , on  $\lambda$  wavelength, for fibres significantly differing in respect of core diameters and numerical apertures. NA means, in our opinion, decrease of the effective defect area which is the splice for  $\lambda = 1550 \text{ nm}$ , i.e., for a mode field diameter MFD bigger then in case of  $1310 \text{ nm}$ .

With the assumption of dopant diffusion within the splice, Fig. 16, for optimised splices “a bigger” it means to

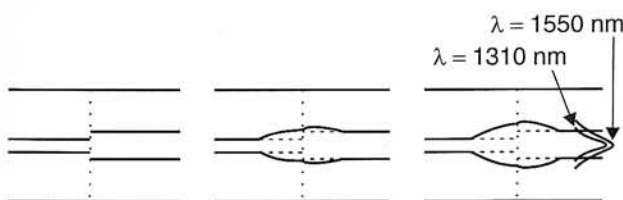


Fig. 16. Arising of transient area in the splice.

a high degree exclusion of cladding, and to a smaller degree exclusion of the core from the defect area which results in smaller splice loss for  $\lambda = 1550 \text{ nm}$ , Fig. 16.

## 7. Conclusion

Standard splicing condition, for II basic step, of SMF one mode fibres with comparable core diameters and numerical apertures which means comparable mode field, for a fusion splicer FSU 925 RTC and FSU 975 are:  $t_2 = 2 \text{ s}$ ,  $I_2 = 15\text{--}16.3 \text{ mA}$ . According to Figs. 10–11 these conditions are not sufficient for fibres which significantly differ with NA and  $2a$ . Then, fibre loss is  $A \approx 0.12\text{--}0.6 \text{ dB}$ . Thus obtaining splices with the loss, which is required in telecommunication  $\leq 0.08 \text{ dB}$  for II and III optical window requires splicing times  $t_2 \geq 4 \text{ s}$  and currents  $I_2 \geq 17 \text{ mA}$ , Figs. 12–14. This result for splicing times corresponds with the results achieved during optimisation process of the intermediate area, Figs. 5–9. It ascertains the loss measurement convergence for II and III optical windows with  $t_2 \geq 4 \text{ s}$  and  $I_2 \geq 17 \text{ mA}$ , Figs. 13–14. Finally, in order to obtain small loss for fibres, which significantly differ in respect of core diameter and numerical apertures (i.e., also in respect of mode field  $MF = 2\omega = 2a/\sqrt{\ln[ka(NA)]}$ ) the middle, basic splicing step should be characterised by the following parameters:  $t_2 \geq 4 \text{ s}$  and  $I_2 \geq 17 \text{ mA}$ .

An indirect conclusion is also a statement of the fact that for non-optimised and optimised (to a smaller degree) single mode splice which significantly differ with NA and  $2a$  the loss of these connections is smaller for  $\lambda = 1550 \text{ nm}$ , than for  $\lambda = 1310 \text{ nm}$ . It is an opposite result than case of splicing single mode fibres with comparable NA and  $2a$ .

## Acknowledgements

The work was financed by a grant of the State Committee for Scientific Research No 8T11 D00613.

## References

1. W. Zheng, “The real time control technique for EDF splicing”, *Ericsson Rev.* **1**, 24 (1993).
2. J.W. Fleming, “Material dispersion in lightguide glasses”, *Electron. Lett.* **11**, 326 (1978).
3. J.W. Fleming and D. L. Wood, “Refractive index dispersion and related properties in fluorine doped silica”, *Appl. Opt.* **19**, 3102 (1983).
4. R.Th. Kerstein, *Einführung in die Optische Nachrichtentechnik*, Springer-Verlag, Berlin, 1983.
5. M. Ratuszek, J. Majewski, Z. Zakrzewski, and J. Zalewski, “Examination of spliced telecommunication fibres of the NZDS-SMF type adjusted to wavelength division multiplexing”, *Optica Appl.* **1–2**, (1999).
6. J. Wójcik, Private information.

7. *User's Manual*, Fusion Splicer FSU 925 RTC, Ericsson, 1992.
8. *User's Manual*, Fusion Splicer FSU 975, Ericsson, 1997.
9. W. Jost, *Diffusion in Solids, Liquids, Gases*, Academic Press, New York, 1960.
10. Fibre Focus – Corning's Materials, 1998.
11. C.M. Miller, S.C. Metter, and I.A. White, *Optical Fibre Splices and Connectors*, Marcel Dekker Inc., New York and Basel, 1986.